

The tube outside is instrumented with six T-type sheathed thermocouples. The thermocouples are brazed on the sides of the tube. The water temperatures are measured with six sheathed T-type thermocouples that places vertically at a corner of the inside tank. All thermocouples are calibrated at a saturation value (100 °C since all tests were done at atmospheric pressure). To measure and/or control the supplied voltage and current, power supply systems are used.

After the water tank is filled with water until the initial water level reaches 1.1 m, the water is, then, heated using four pre-heaters at constant power. When the water temperature is reached the saturation value, the water is then boiled for 30 minutes to remove the dissolved air. The temperatures of the tube surfaces are measured when they are at steady state while controlling the heat flux on the upper tube surface (q_T'') with input power. The degree of a wall superheating (ΔT_{sat}) is calculated by subtracting the liquid saturation temperature from the tube surface temperature.

The uncertainties of the experimental data are calculated from the law of error propagation [5]. The uncertainty of the measured temperature has the value of $\pm 0.11^\circ\text{C}$. The uncertainty in the heat flux is estimated to be $\pm 0.7\%$. Since the values of the heat transfer coefficient are the results of the calculation of $q_T''/\Delta T_{sat}$, a statistical analysis on the results is performed. After calculating and taking the mean of the uncertainties of the propagation errors, the uncertainty of the heat transfer coefficient is determined to be $\pm 6\%$.

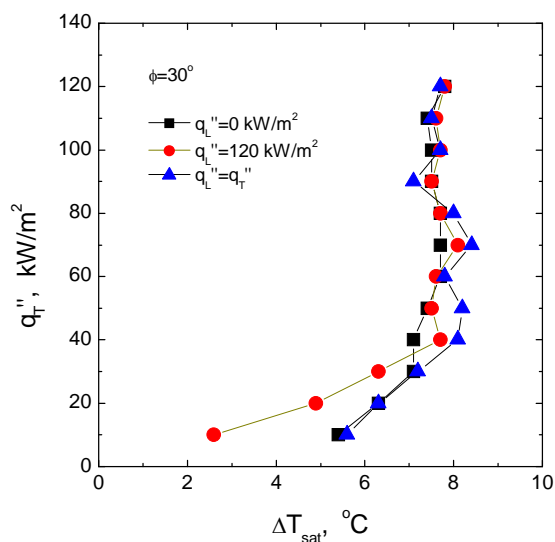


Fig. 3. Plots of q_T'' versus ΔT_{sat} .

3. Results

Figure 3 shows plots of q_T'' versus ΔT_{sat} data obtained from the experiments. Three heat fluxes of the lower tube are tested for $\phi=30^\circ$. As shown in the figure, the heat transfer on the upper tube is enhanced when $q_L''=120\text{kW/m}^2$ and $q_T'' \leq 30\text{kW/m}^2$ comparing to the single tube (i.e., $q_L''=0\text{kW/m}^2$). The change of q_L'' from

120 to 0kW/m^2 results in 107.7% (from 2.6 to 5.4°C) increase of ΔT_{sat} when $q_T''=10\text{kW/m}^2$. When $q_L''=q_T''$, the heat transfer of the upper tube is deteriorating comparing to the single tube at moderate heat fluxes. However, the curves for $q_L'' \neq 0\text{kW/m}^2$ converge to the curve for the single tube when $q_T'' > 40\text{kW/m}^2$.

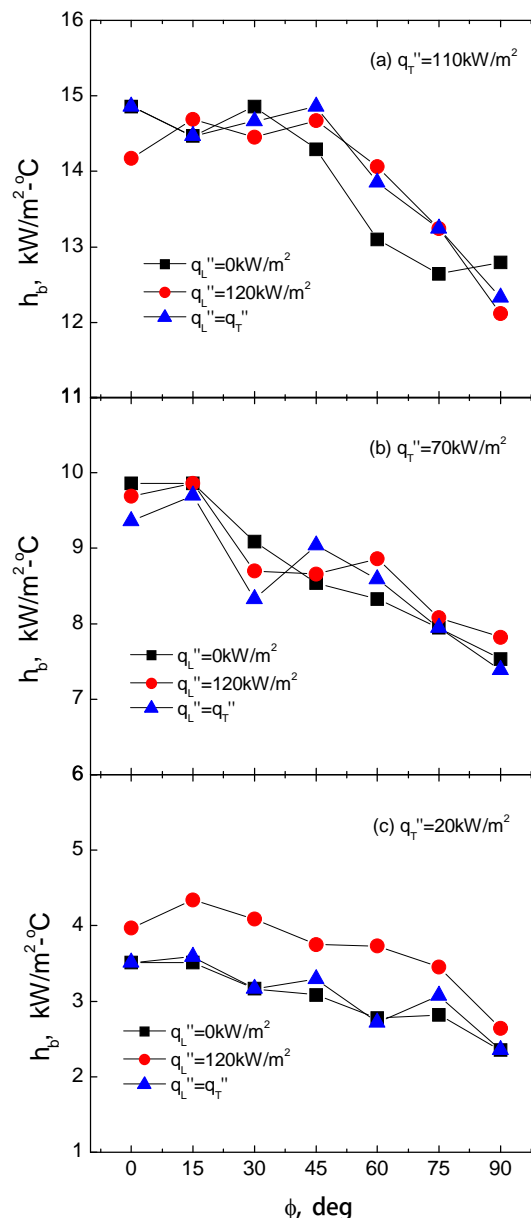


Fig. 4. Variation in heat transfer coefficient against inclination angle for different heat fluxes.

The variation of the heat transfer coefficient due to the inclination angle change is plotted in Fig. 4 for the different heat fluxes (q_T'' and q_L''). Through the heat fluxes, the increase of the inclination angle eventually decreases heat transfer coefficients. As the inclination angle increases the affected region by the bubbly flow from the lower tube becomes reducing, and this causes the decrease in the heat transfer. The curve for $q_L''=120\text{kW/m}^2$ and q_T'' shows enhanced heat transfer

coefficient comparing to the single tube. As the inclination angle increases, the local pitches (P_1 and P_2) are changing. Since the affected area of the convective flow gets broadened and the intensity becomes weaker as P/D increases, the enhancement is observed great when the pitch is not large [6]. As the pitch increases over a critical value, the heat transfer of the upper tube becomes insensitive to the one [6]. As the inclination angle increases, part of the tube has a region of smaller local pitches than the average one. This region causes the enhancement in heat transfer. When $q_T''=20\text{kW/m}^2$ and q_L'' is high, the intensity of the convective flow gets stronger. When $q_T''=110\text{kW/m}^2$, the effect of bubble dynamics gets dominant. Therefore, enhanced heat transfer is observed for the curves of $q_L''=120\text{kW/m}^2$ and q_T'' at these heat fluxes. However, no visible enhancement in heat transfer is observed among the three cases of q_L'' when $q_T''=70\text{kW/m}^2$.

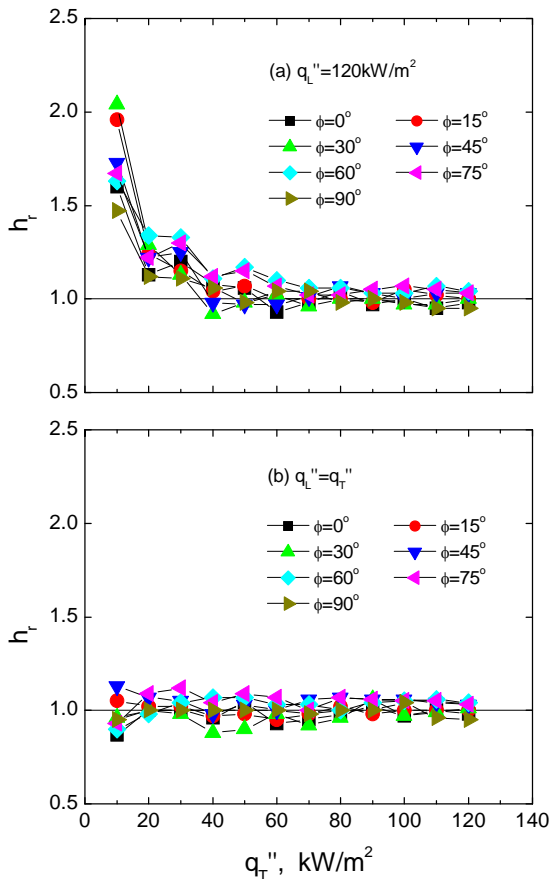


Fig. 5. Plots of h_r versus q_T'' for different inclination angles.

The bundle effect is expected as the convective flow of bubbles and liquid, rising from the lower tube, enhances the heat transfer on the upper tube [7]. The increase in q_L'' results in the stronger intensity of the convective flow. The heat transfer on the upper tube is associated with (1) the bulk movement of bubble and liquid coming from the lower side and (2) micro-convective component relates to the heat transfer associated with the bubble nucleation and growth on the tube surface [8].

Figure 5 shows variations in the bundle effect against the heat flux of the upper tube for $q_L''=120\text{kW/m}^2$ and q_T'' . As the heat flux of the upper tube increases, the bundle effect decreases dramatically. The maximum bundle effect is observed at $q_T''=10\text{kW/m}^2$. Significant bundle effect has been found at q_T'' is less than 60kW/m^2 . However, the bundle effect converges to unity at higher heat fluxes regardless of the heat flux of the lower tube. When $\phi=15^\circ$ and 30° higher bundle effect is observed comparing to the other inclinations. For the angles, the affected region is not much reduced, and the bubble dynamics is stronger compared to the single tube. These phenomena lead to the increase in the bundle effect. However, the gradual increase in the inclination angle results in the reduction of the affected region and this causes the deterioration in the bundle effect.

4. Conclusions

An experimental study is performed to investigate the combined effects of an inclination angle of the upper tube and the heat flux of the lower one on pool boiling heat transfer of the upper one. Through the study, two smooth stainless steel tubes of 19mm diameter and 400mm length are tested in the water at atmospheric pressure. The major conclusions of the present study are as follows:

- (1) Through the heat fluxes, the increase of the inclination angle eventually decreases heat transfer coefficients because the affected region by the bubbly flow from the lower tube becomes reducing.
- (2) Significant bundle effect has been found at q_T'' is less than 60kW/m^2 . The enhancement is clearly observed at the heat fluxes where the convective effect is dominant.

REFERENCES

- [1] S. B. Memory, S. V. Chilman, P. J. Marto, Nucleate Pool Boiling of a TURBO-B Bundle in R-113, ASME J. Heat Transfer, Vol. 116, p. 670, 1994.
- [2] A. Swain, M. K. Das, A Review on Saturated Boiling of Liquids on Tube Bundles, Heat Mass Transfer, Vol. 50, p. 617, 2014.
- [3] Z.-H. Liu, Y.-H. Qiu, Enhanced Boiling Heat Transfer in Restricted Spaces of a Compact Tube Bundle with Enhanced Tubes, Applied Thermal Engineering, Vol. 22, p. 1931, 2002.
- [4] M. G. Kang, Pool Boiling Heat Transfer from an Inclined Tube Bundle, Int. J. Heat Mass Transfer, Vol. 101, p. 445, 2016.
- [5] H.W. Coleman, W.G. Steele, Experimentation and Uncertainty Analysis for Engineers, 2nd Ed., John Wiley & Sons, 1999.
- [6] M. G. Kang, Pool Boiling Heat Transfer on Tandem Tubes in Vertical Alignment, Int. J. Heat Mass Transfer, Vol. 87, p. 138, 2015.
- [7] E. Hahne, Chen Qui-Rong, R. Windisch, Pool Boiling Heat Transfer on Finned Tubes –an Experimental and Theoretical Study, Int. J. Heat Mass Transfer, Vol. 34, p. 2071, 1991.
- [8] A. Gupta, J. S. Saini, H. K. Varma, Boiling Heat Transfer in Small Horizontal Tube Bundles at Low Cross-Flow Velocities, Int. J. Heat Mass Transfer, Vol. 38, p. 599, 1995.